

# SCIENTIFIC REPORTS



OPEN

## Epitopes of anti-RIFIN antibodies and characterization of *rif*-expressing *Plasmodium falciparum* parasites by RNA sequencing

Received: 03 November 2016

Accepted: 20 January 2017

Published: 24 February 2017

Jun-Hong Ch'ng<sup>1,2</sup>, Madle Sirel<sup>1,\*</sup>, Arash Zandian<sup>3,\*</sup>, Maria del Pilar Quintana<sup>1,\*</sup>, Sherwin Chun Leung Chan<sup>1,\*</sup>, Kirsten Moll<sup>1,\*</sup>, Asa Tellgren-Roth<sup>4,\*</sup>, IngMarie Nilsson<sup>4</sup>, Peter Nilsson<sup>3</sup>, Ulrika Qundos<sup>3</sup> & Mats Wahlgren<sup>1</sup>

Variable surface antigens of *Plasmodium falciparum* have been a major research focus since they facilitate parasite sequestration and give rise to deadly malaria complications. Coupled with its potential use as a vaccine candidate, the recent suggestion that the repetitive interspersed families of polypeptides (RIFINs) mediate blood group A rosetting and influence blood group distribution has raised the research profile of these adhesins. Nevertheless, detailed investigations into the functions of this highly diverse multigene family remain hampered by the limited number of validated reagents. In this study, we assess the specificities of three promising polyclonal anti-RIFIN antibodies that were IgG-purified from sera of immunized animals. Their epitope regions were mapped using a 175,000-peptide microarray holding overlapping peptides of the *P. falciparum* variable surface antigens. Through immunoblotting and immunofluorescence imaging, we show that different antibodies give varying results in different applications/assays. Finally, we authenticate the antibody-based detection of RIFINs in two previously uncharacterized non-rosetting parasite lines by identifying the dominant *rif* transcripts using RNA sequencing.

The function of repetitive interspersed families of polypeptides (RIFINs) in blood group A-specific rosetting has generated much interest concerning the importance of malaria in shaping geographical blood group profiles<sup>1</sup>. However, the number (150–200 copies per haploid genome) and diversity of this multigene copy family suggests that the characteristics of these proteins are likely to be highly varied<sup>2–5</sup>.

RIFINs have been classified into two subgroups, with 70% belonging to subgroup A (A-RIFINs), possessing a 25 amino acid insertion-deletion (indel) region, and 30% to subgroup B (B-RIFINs) which lack an indel<sup>3</sup>. During the trophozoite stages, A-RIFINs have been shown to be exported to the host cell membrane while B-RIFINs remain within the parasite<sup>3,6–8</sup>. RIFINs have also been shown to be expressed in sporozoite, merozoite and gametocyte stages although their functions there have yet to be elucidated<sup>8–10</sup>.

Rosettes are formed when an infected erythrocyte (iRBC) binds to uninfected erythrocytes (uRBCs) to form cell clusters which then occlude microvasculature and lead to malaria complications. The rosettes formed by blood group A erythrocytes are of clinical significance because individuals with blood group A are more likely to develop severe malaria compared to blood group O<sup>11–17</sup>. Rosettes of this blood group have been demonstrated to have stronger binding<sup>18</sup>, be resistant to heparin-induced dispersion<sup>19</sup> and even to shield the iRBC from antibody binding<sup>20</sup>.

Another report on broadly reactive human anti-RIFIN antibodies has also generated much discussion about the potential for RIFINs as vaccine candidates<sup>21</sup>. Spontaneously occurring LAIR1 insertions between V and DJ

<sup>1</sup>Department of Microbiology, Tumor and Cell Biology (MTC), Karolinska Institutet, Stockholm, Sweden.

<sup>2</sup>Department of Microbiology and Immunology, National University of Singapore, Singapore. <sup>3</sup>Affinity Proteomics, Science for Life Laboratory, School of Biotechnology, Royal Institute of Technology (KTH), Stockholm, Sweden.

<sup>4</sup>Center for Biomembrane Research, Department of Biochemistry and Biophysics, Stockholm University, Stockholm, Sweden. \*These authors contributed equally to this work. Correspondence and requests for materials should be addressed to J.-H.C. (email: junhong.chng@ki.se) or M.W. (email: mats.wahlgren@ki.se)

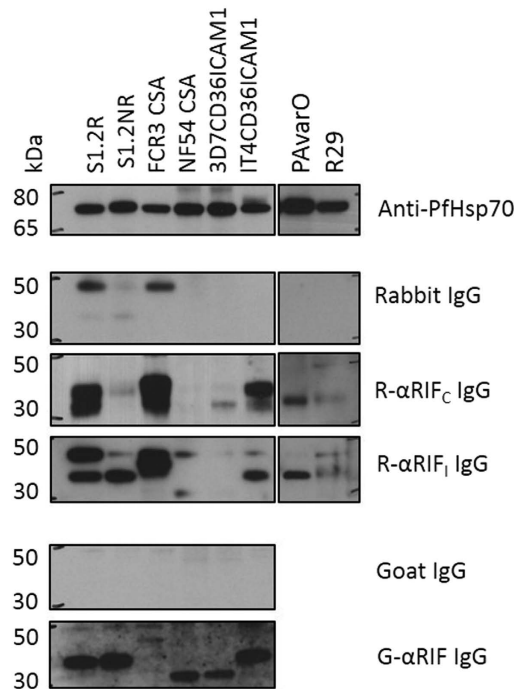


**Figure 1. Western blots of RIFINs in multiple parasite strains.** SDS-extracted parasite lysates of S1.2R, S1.2NR, FCR3CSA, NF54CSA, 3D7CD36ICAM1 and IT4CD36ICAM1 were run on SDS-PAGE (lanes 1–6 respectively), transferred to nitrocellulose membrane and blotted with rabbit anti-PfHsp70 (1:2000), non-immune rabbit IgG (10 µg/ml), R $\alpha$ RIF<sub>C</sub> (rabbit anti-A-RIFIN C-terminus) IgG (10 µg/ml), R $\alpha$ RIF<sub>I</sub> (rabbit anti-A-RIFIN indel) IgG (10 µg/ml), non-immune goat IgG (10 µg/ml) and G $\alpha$ RIF (goat anti-A-RIFIN full length) IgG (10 µg/ml). Corresponding HRP-conjugated secondary anti-rabbit and anti-goat IgG antibodies were used together with ECL reagent for detection. Description of the antigens used for immunizations of R $\alpha$ RIF<sub>C</sub>, R $\alpha$ RIF<sub>I</sub> and G $\alpha$ RIF are described in Supplementary Table S1 and diagrammatically illustrated in Fig. 3D.

segments gave rise to a 98 amino acid collagen-binding domain insertion that resulted in broadly neutralizing antibodies directed towards the RIFINs on the iRBC surface.

With the great promise for medical advances captured by these early findings, it is fundamental to assess the quality of available reagents to assay for RIFINs. Thus far, most studies on RIFINs make use of techniques like surface iodination or antibody-based assays (western blotting, immunofluorescence microscopy, flow cytometry, immunoprecipitation etc.) to study the presence, localization or function of RIFINs in the parasite<sup>1,7,10,21–27</sup>. The specificities of such approaches are limited and are only occasionally backed with more unambiguous methods like GFP-tagged over-expression models or MALDI-TOF identification of immuno-precipitated proteins. To the best of our knowledge, anti-RIFIN antibody profiling is never performed though these reagents are linchpins to study claims. As described recently<sup>28,29</sup>, the lack of thorough antibody validation will inadvertently lead to experimental results that are irreproducible, confusing or untrue.

In this study, we make use of ultra-dense peptide arrays to examine the specificities of anti-RIFIN IgG preparations, test the functionality of these antibodies in different antibody-based assays, and finally follow up with RNA sequencing (RNAseq) to determine RIFIN expression in laboratory-adapted parasite lines. In conclusion, we describe the assay-specific utility of the antibodies, the potential for cross-reactivity, and also identify the dominant RIFINs on two non-rosetting parasite lines.

## Results

**Western blots.** Several techniques were used to characterize anti-RIFIN antibodies. To begin, purified IgG from 10 rabbits (R $\alpha$ RIF<sub>C</sub>, R2 $\alpha$ RIF<sub>C</sub>, R3 $\alpha$ RIF<sub>C</sub>, R4 $\alpha$ RIF<sub>C</sub>, R5 $\alpha$ RIF<sub>C</sub>, R6 $\alpha$ RIF<sub>C</sub>, R7 $\alpha$ RIF<sub>C</sub>, R8 $\alpha$ RIF<sub>C</sub>, R $\alpha$ RIF<sub>I</sub> and R2 $\alpha$ RIF<sub>I</sub>) and 1 goat (G $\alpha$ RIF) that had been immunized with RIFIN peptides/protein (Supplementary Table S1) were tested in Western blots of SDS extracts of S1.2R, a well-studied rosetting parasites strain that is RIFIN-positive (results not shown). Only antibodies from R $\alpha$ RIF<sub>C</sub>, R $\alpha$ RIF<sub>I</sub> and G $\alpha$ RIF resulted in bands of the expected size of approximately 35 kDa (Fig. 1). Together with the relevant commercial non-immune IgG to exclude non-specific staining and anti-Hsp70 to ensure similar loading (Fig. 1), these three reactive IgG preparations were used to detect the presence of RIFINs in other laboratory strains including FCR3CSA, NF54CSA, 3D7CD36ICAM1, IT4CD36ICAM1, PavarO and R29.

Western blot staining with R $\alpha$ RIF<sub>C</sub> IgG (rabbit immunized with the conserved A-RIFIN C-terminal peptide, see Fig. 3D) showed prominent bands with sizes corresponding to the RIFINs (between 30–40 kDa) in S1.2R, FCR3CSA, IT4CD36ICAM1 and to a lesser extent in PavarO (Fig. 1 and Supplementary Figure S1). In these lysates, the presence of two bands between 35–45 kDa was noted for S1.2R and FCR3CSA. Several faint bands at

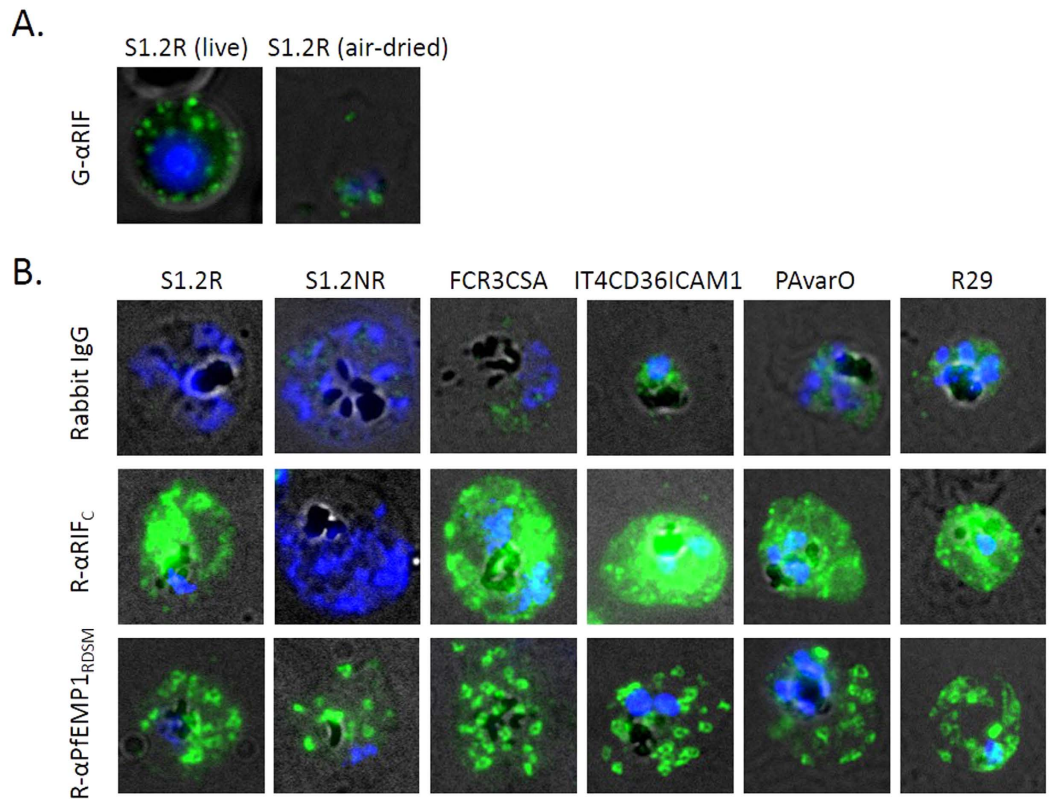


**Figure 2. Indirect immunofluorescence micrographs.** (A) G $\alpha$ RIF IgG labelling of RIFINs on a live S1.2R-infected erythrocyte and an air-dried iRBC. (B) Air-dried monolayers of erythrocytes infected with S1.2R, S1.2NR, FCR3CSA, IT4CD36ICAM1, PAvarO and R29 parasites stained with non-immune rabbit IgG (10  $\mu$ g/ml), anti-RIFIN R $\alpha$ RIF<sub>C</sub> rabbit IgG (10  $\mu$ g/ml) and Maurer's cleft labelling by R- $\alpha$ PfEMP1<sub>RD5M</sub> IgG (8  $\mu$ g/ml). Alexa488-conjugated secondary anti-rabbit or anti-goat antibodies were used (1:200) as well as Vectashield with DAPI (nuclear staining). Merged channels of transmission light (black and white), green (Alexa 488) and blue (DAPI) and representative cells are shown here.

higher molecular weights could also be observed and were likely due to some limited degree of cross-reactivity (Supplementary Figure S1).

Staining with R $\alpha$ RIF<sub>1</sub> IgG (rabbit immunized with a conserved A-RIFIN indel peptide, see Fig. 3D) showed that A-RIFINs were expressed in S1.2R, FCR3CSA, IT4CD36ICAM1 and PAvarO, but also to some degree in S1.2NR and R29 (Fig. 1 and Supplementary Figure S1). Again, some faint bands could again be seen (in S1.2R > 185 kDa and in FCR3CSA at 115 kDa and >185 kDa) and may indicate some cross reactivity to higher molecular weight proteins (Supplementary Figure S1).

IgG purified from G $\alpha$ RIF (goat immunized with full-length PF3D7\_0100400, see Fig. 3D) showed prominent bands at about 35 kDa for S1.2R, S1.2NR and IT4CD36ICAM1 (Fig. 1). While there was only a single clear band for S1.2R, there were multiple prominent bands at 30, 50, 60, 80, 115 and 185 kDa in extracts of other parasite lines (Supplementary Figure S1) indicating significant cross-reactivity with other parasite proteins in these parasites.

**Indirect Immunofluorescence Assay.** G $\alpha$ RIF IgG had previously been used to label live S1.2R parasites for cytometry<sup>1</sup> and its reactivity has been very specific – no other laboratory strain or field isolate tested to date have shown any surface staining (results not shown). Unlike the antibody labeling of live S1.2R-infected cells which showed punctate surface-specific staining (Fig. 2A, left panel), air dried monolayers stained with G $\alpha$ RIF IgG showed only a faint parasite cytoplasmic staining (Fig. 2A, right panel) suggesting that the native conformational (3D) epitope may have been lost during the fixing by desiccation. Higher antibody concentrations resulted in non-specific staining of even the uninfected RBCs (data not shown) and did not improve detection.

Since desiccation results in breaks in the membrane and exposes the inner surface of the RBC membrane where the conserved RIFIN C-terminus is located, R $\alpha$ RIF<sub>C</sub> IgG could readily label S1.2R-infected RBCs in a patchy manner (Fig. 2B). In comparison, IgG from R $\alpha$ RIF<sub>1</sub>, R5 $\alpha$ RIF<sub>C</sub> and R6 $\alpha$ RIF<sub>C</sub> showed no notable staining (data not shown). R $\alpha$ RIF<sub>C</sub> IgG was then applied to air-dried monolayers of other parasite strains to detect and localize potential A-RIFINs. While S1.2NR (Fig. 2B), NF54CSA and 3D7CD36ICAM1 (data not shown) had no notable staining, FCR3CSA, IT4CD36ICAM1, PAvarO and R29 parasites showed staining similar to S1.2R (Fig. 2B).

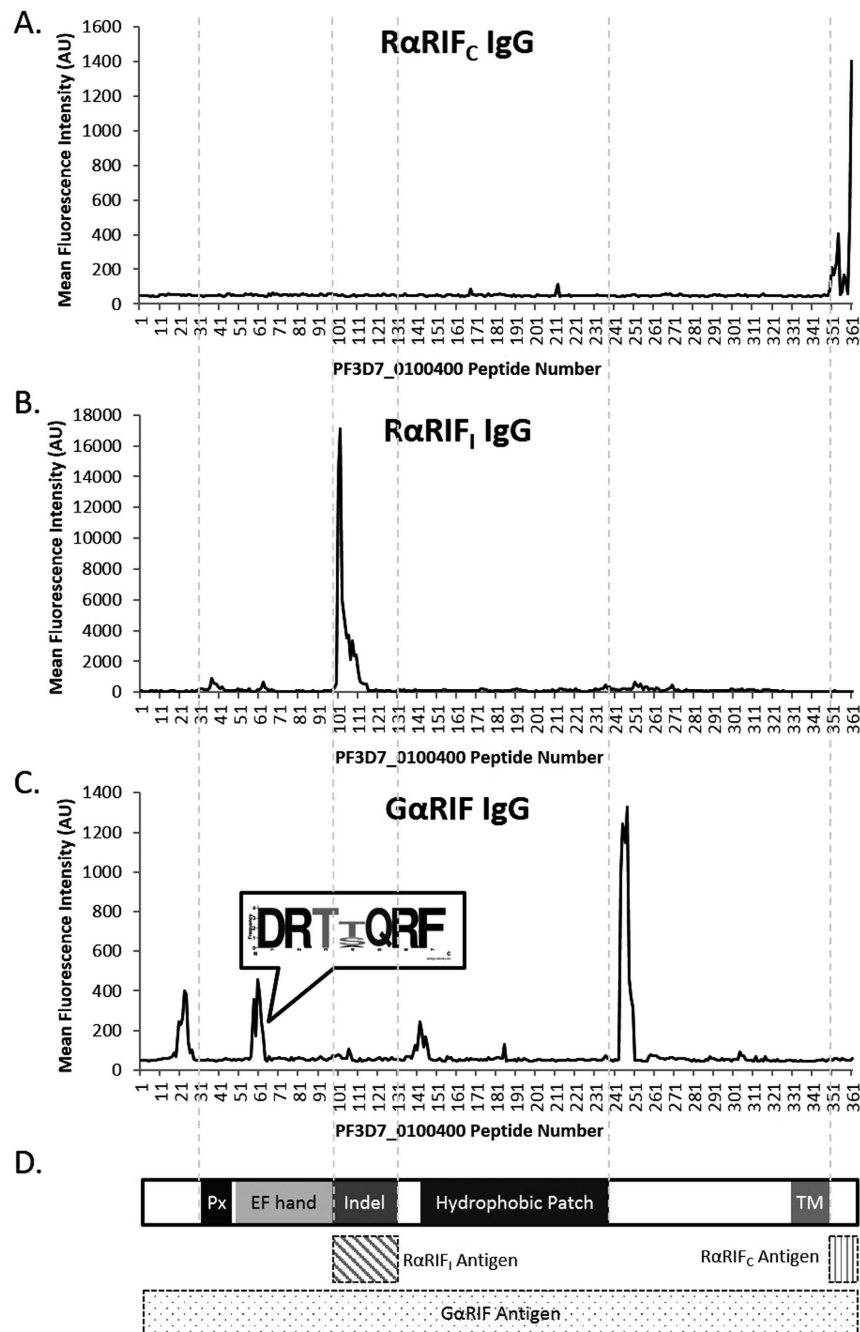


**Figure 3. Epitope region mapping of anti-RIFIN antibodies using an ultra-dense peptide array.** The reactivity for polyclonal IgG purified from (A) RαRIF<sub>c</sub>, (B) RαRIF<sub>i</sub> and (C) GαRIF are shown here against peptides from the RIFIN protein PF3D7\_0100400. Y-axis shows mean median fluorescence intensity of duplicate spots and X-axis shows the peptide number from the N terminus to the C-terminus. (C) A conserved amino acid sequence that is recognized by GαRIF IgG is highlighted. (D) A diagram of RIFIN PF3D7\_0100400 domains is provided together with the respective antigens used for immunizations: RαRIF<sub>c</sub> was immunized with the C-terminus, RαRIF<sub>i</sub> with the indel region and GαRIF with the full length of PF3D7\_0100400. The abbreviation “Px” stands for PEXEL motif while “TM” refers to the transmembrane domain. Detailed intensity plots of the key epitope regions are highlighted in Supplementary Figure S2.

The staining by RαRIF<sub>c</sub> IgG was markedly different from that of R-αPfEMP1<sub>RDSM</sub> IgG, which stained all the six tested parasites with distinct “donut” shapes (Fig. 2B). This strain-transcending rabbit αPfEMP1<sub>RDSM</sub> (respiratory distress severe malaria) antibody has been described before as staining the Maurer’s clefts though binding the RDSM peptide of PfEMP1 that is only exposed *en route* to the RBC surface<sup>30</sup>. In comparison, non-immune rabbit IgG at the same concentration showed little or no staining of the air-dried monolayers (Fig. 2B).



**Epitope region mapping by peptide array.** An ultra-dense peptide array was used to epitope map anti-RIFIN polyclonal IgG antibodies purified from the sera of two non-immune and five immunized animals (R $\alpha$ RIF<sub>C</sub>, R5 $\alpha$ RIF<sub>C</sub>, R6 $\alpha$ RIF<sub>C</sub>, R $\alpha$ RIF<sub>I</sub>, and G $\alpha$ RIF). The peptide array contained 12 amino acid fragments of parasite surface antigens including PfMC-2TM, PHIST, RIFIN, STEVOR, SURFIN and several PfEMP1 proteins, with an 11-residue overlap between peptides derived from the same protein.

Background binding was minimal: the non-immune rabbit IgG reacted with 7 of the 443 arrayed proteins (reactivity scores of 2 or 3) and non-immune goat IgG reacted with only one protein (reactivity score of 2).

The IgG of R $\alpha$ RIF<sub>C</sub>, immunized with the conserved 20 amino acid C-terminal peptide of A-RIFINs, showed that about half of the RIFINs (141/278) were bound at the C-terminus after the transmembrane (TM) segment with a most frequent reactivity score of 6 (Supplementary Data S1). Of these 141 RIFINs, R $\alpha$ RIF<sub>C</sub> gave a reactivity score of 8 for PF3D7\_0100400, with the 8 peptides spread across three epitope regions (Fig. 3A and Supplementary Figure S2A). Several SURFINs and STEVORs also showed reactivity, but R $\alpha$ RIF<sub>C</sub> had no reactivity against any of the arrayed PfEMP1s, PHISTs or PfMC2TMs.

Both R5 $\alpha$ RIF<sub>C</sub> and R6 $\alpha$ RIF<sub>C</sub> were immunized with the conserved B-RIFIN C-terminus. However, IgG of both rabbits had a higher reactivity score for many of the short-listed PfEMP1s than the RIFINs (Supplementary Data S1). There was also significant cross-interaction with SURFIN and PHIST peptides which limited the utility of these unspecific antibodies.

R $\alpha$ RIF<sub>I</sub>, immunized with the semi-conserved indel region of A-RIFINs, bound a third of the RIFINs (102/278) with reactivity scores around 3 to 11 (Supplementary Data S1). Most of these RIFINs that reacted were a subset of those detected by R $\alpha$ RIF<sub>C</sub> IgG and binding was generally localized to the indel region. In PF3D7\_0100400, R $\alpha$ RIF<sub>I</sub> recognized 13 peptides that were confined within one epitope region (Fig. 3B and Supplementary Figure S2B). There was a limited degree of cross-reactivity to a few other members from surface antigen families.

G $\alpha$ RIF was immunized with full length A-RIFIN PF3D7\_0100400 and had a reactivity score of 23 against the peptides of this same protein (Supplementary Data S1). Closer inspection of the peptide-intensity plot of this 372 amino acid sequence revealed five main epitopes regions (Fig. 3C and Supplementary Figure S2C): a sequence upstream of the PEXEL motif (NTHKKPSITSRHIQTTR –unique to PF3D7\_0100400), a sequence in the first half of the EF hand region (MQQFHDRITQRFHEYDE), two adjoining sequences at the start of the hydrophobic patch (QNLGKIVAPSSGVLG –unique to PF3D7\_0100400) and a final region just after the hydrophobic patch (PSLVNDQLVGTENTSDPF –unique to PF3D7\_0100400). Of the 436 bona fide peptides G $\alpha$ RIF reacted towards, 336 peptides coming from 52 RIFINs contained the sequence D-R-T-T/S/A-Q-R-F (Fig. 3C insert and Supplementary Data S1). In total, G $\alpha$ RIF IgG reacted with a quarter of all the RIFINs on the array (66/278) of which most had a reactivity score of 6. Binding to a few members of PfEMP1, SURFINs, STEVORs and PHISTs could also be detected.

**RNA sequencing and qPCR validation.** To characterize RIFIN expression, RNAseq was performed on NF54CSA, S1.2NR, FCR3CSA and IT4CD36ICAM1 parasites at 10, 20, 30 and 40 hours post invasion (hpi), with the exception of S1.2NR at 40 hpi due to failed library preparation. RNAseq was not carried out for PAVarO as its genome is not well curated and not for 3D7CD36ICAM1 or R29 as they did not have high levels of RIFINs as indicated by Western blot.

In NF54CSA and S1.2NR parasites (both negative for RIFINs using R $\alpha$ RIF<sub>C</sub> antibodies) the Reads Per Kilobase of transcript per Million mapped reads (RPKM) of *rif* genes were relatively low (Supplementary Data S2). In NF54CSA, the highest expressed *rifs* were PF3D7\_120050 (239 RPKM at 10 hpi, Supplementary Data S2), PF3D7\_1000600 (188 RPKM at 20hpi), PF3D7\_0732900 (183 RPKM at 20 hpi), PF3D7\_0808900 (129 RPKM at 20 hpi) and PF3D7\_0425900 (103 RPKM at 20 hpi) (Fig. 4A, Supplementary Data S2). In S1.2NR, the highest expressed *rifs* were PFIT\_0411800 (431 RPKM at 20 hpi) and PFIT\_0100200 (190 RPKM at 20 hpi) (Fig. 4B, Supplementary Data S2).

In contrast, the RPKM of the highest expressed *rifs* in FCR3CSA and IT4CD36ICAM1 (both positive for RIFINs using R $\alpha$ RIF<sub>C</sub> antibodies) were markedly higher (Supplementary Data S2). The highest expressed *rif* for FCR3CSA was PFIT\_bin00500 (2693 RPKM at 20 hpi) followed by PFIT\_0536600 (281 RPKM at 20 hpi) and PFIT\_bin07200 (243 RPKM at 20 hpi) (Fig. 4C). At similar levels, the highest expressed *rif* in IT4CD36ICAM1 was PFIT\_0835500 (3273 RPKM at 20 hpi) followed by PFIT\_0733200 (910 RPKM at 20 hpi), PFIT\_0900200 (662 RPKM at 20 hpi) and PFIT\_0900150 (660 RPKM at 20 hpi) (Fig. 4D). Temporally, the peak expression for these two maximally expressed RIFINs in these two parasites was at 20 hpi (Fig. 4E).

To validate the RNAseq results, ten *rif* genes were selected for verification by qPCR using fructose biphosphate aldolase (FBA) as a reference (Fig. 4F). There was a strong correlation (Pearson  $r = 0.8607$ ) between RNAseq and qPCR data from the three tested parasite lines (S1.2NR, FCR3CSA and IT4CD36ICAM1) thereby validating RNAseq quality and confirming that the dominant *rif* transcripts are PFIT\_bin00500 and PFIT\_0835500 for FCR3CSA and IT4CD36ICAM1 respectively.

## Discussion

Despite being the largest multigene family of proteins in *P. falciparum*, the RIFINs have remained poorly characterized and have only come into the research spotlight most recently. Among other factors, the sheer number of genes and the lack of reliable reagents to assay these proteins have hampered advances in this field of research.

Previous attempts to generate high quality antibodies had limited success. For example, we had tried to generate mice hybridomas (to get monoclonal antibodies) by first immunizing 6 mice with the near-full length PF3D7\_0100400 protein (amino acid 30-329), 6 mice with a semi-conserved A-RIFIN N-terminal peptide (PSNYDNDPEMKEVMQ), 3 mice with a conserved B-RIFIN N-terminal peptide (FDRQTSQRFEYEER) and 3 mice with A-RIFIN C-terminus (LRYRRKKKMKKKLQYIKLL). Although positive to the antigens by ELISA, none of the resulting antisera were reactive against S1.2R parasites by live cell surface staining (native

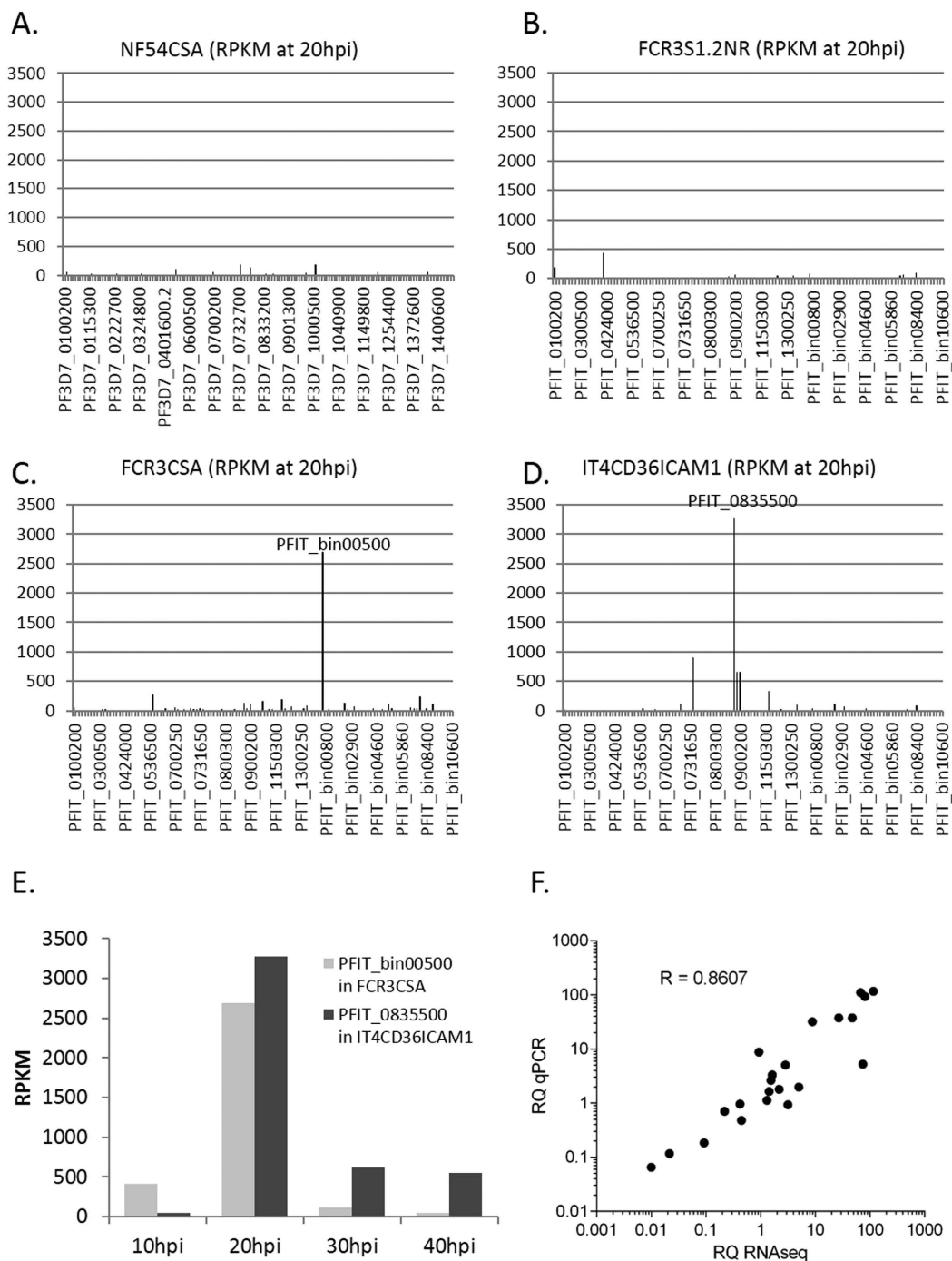


**Figure 4. RNA sequencing counts of *rif* genes.** RNA from (A) NF54CSA, (B) S1.2NR, (C) FCR3CSA and (D) IT4CD36ICAM1 were extracted at four time points and sent for RNA sequencing. Results for the *rif* genes are presented here in RPKM at 20 hpi. (E) RPKM values at 10, 20, 30 and 40 hpi are provided to show the temporal expression of the two dominant *rif* genes (PFIT\_bin00500 in FCR3CSA and PFIT\_0835500 in IT4CD36ICAM1). (F) Quantitative real time PCR was performed to validate the RNA sequencing results and Pearson's R shows level of correlation between the relative quantity (RQ) of qPCR fold expression and RNAseq RPKM values.

extracellular epitopes), IFA (fixed extracellular and intracellular epitopes) or Western blot (linearized epitopes) (results not shown).

Another series of immunizations in ten rabbits and one goat yielded some RIFIN-reactive antisera, some of which were published previously<sup>1</sup>. In the present study we apply these reagents to multiple laboratory parasite strains and map the epitopes of these anti-RIFIN antibodies.

Of the polyclonal IgG purified from sera of these eleven animals, only three ( $R\alpha RIF_C$ ,  $R\alpha RIF_I$  and  $G\alpha RIF$ ) gave western blot bands corresponding to the expected size of the dominant RIFIN in FCR3S1.2 (PFIT\_bin05750 predicted to be 37.1 kDa). These antibodies were then tested on the SDS extracted lysates of seven other strains (S1.2NR, NF54CSA, FCR3CSA, 3D7CD36ICAM1, IT4CD36ICAM1, PAvarO and R29) but with inconsistent results. Some lysates had bands from all three antibodies; others had no bands, while some showed bands only for one or two of the antibodies. The inconsistencies are perhaps unsurprising since the polyclonal antibodies were raised against different epitopes. Even if RIFINs are being expressed, they may or may not have the same epitopes and as such may not be recognized by the antibodies. Also, the appearance of multiple close bands had also been described before<sup>1</sup> but the reason for this has yet to be uncovered. Since the specificity of the antibodies had yet to be ascertained at this stage, we could only conclude tentatively that S1.2R, S1.2NR, FCR3CSA, IT4CD36ICAM1, PAvarO and R29 might contain RIFINs while NF54CSA and 3D7CD36ICAM1 had no detectable RIFINs.

In immunofluorescence staining, only one of these three antibodies ( $R\alpha RIF_C$ ) gave a positive signal to S1.2R parasites. When applied to the same seven parasite strains as before, iRBC membrane staining could be identified in FCR3CSA, IT4CD36ICAM1, PAvarO and R29 but not in S1.2NR, NF54CSA or 3D7CD36ICAM1. The pattern of localization of all five positively-stained parasites closely resembled each other with patchy staining of the iRBC surface. The staining was markedly different from the characteristic donut-shaped pattern observed by staining of the Maurer's clefts<sup>30</sup> and appears contrary to previous findings that indicate RIFIN export via the Maurer's clefts<sup>24,25,27</sup>. The difference in staining may be because of sub-detectable levels of RIFINs located in the Maurer's clefts at the point of staining, because the compartmentalization of RIFINs within the Maurer's clefts are unique in different parasites, or possibly because the RIFINs of these parasites are trafficked to the RBC surface without passing through the Maurer's clefts. However, it is difficult to draw conclusions since co-staining was not performed (both  $R\alpha PfEMP1_{RDSM}$  and  $R\alpha RIF_C$  are rabbit IgG making co-staining challenging) and once again, the specificity of  $R\alpha RIF_C$  IgG could be called into question. As such, peptide arrays were utilized to determine the specificity of the three most promising antibodies and provide information on their targeted epitopes.

An ultra-dense peptide array was designed to contain peptides spanning most of the known *P. falciparum* surface antigens. Of the anti-RIFIN antibodies tested,  $R\alpha RIF_C$  was the most specific for the RIFINs, binding to the conserved C-terminus of half of the tested RIFINs and not to many other peptides on the array. This suggests that  $R\alpha RIF_C$  antibodies have high specificity for RIFINs since cross-reactivity to other tested surface antigens is nominal, at least at the level of the primary amino acid sequence. Western blots of the parasite SDS extract also had no prominent bands outside of the 35–45 kDa region, further supporting the specificity of  $R\alpha RIF_C$  IgG to the RIFINs. Importantly, the peptide array indicated that  $R\alpha RIF_C$  IgG should have a 50% likelihood of detecting a randomly expressed RIFIN - a considerable percentage given the variability of the RIFINs. Implicitly, it also does mean that there is a 50% chance that a RIFIN-expressing parasite would be missed as a false negative. However,  $R\alpha RIF_C$  antibodies are not useful for functional assays (they cannot be used to block the function of the protein in inhibition assays) since the binding is specific to the intracellular C-terminus and there is therefore a requirement for cells to first be fixed and permeabilized.

$R\alpha RIF_I$  antibodies also demonstrated good specificity for RIFINs based on the peptide array, with binding primarily targeting the indel regions of a third of all RIFINs arrayed. Although this region is predicted to be extracellular,  $R\alpha RIF_I$  showed no binding to live iRBC surface of S1.2, FCR3CSA, IT4CD36ICAM1, PAvarO or R29. Since  $R\alpha RIF_I$  was able to give prominent bands to lysates of those same parasites by Western blot, this may suggest that the epitope is hidden in the native protein conformation and only accessible to antibody binding when linearized. This thereby renders  $R\alpha RIF_I$  antibodies unsuitable for functional studies as well.

The only functional anti-RIFIN antibody at our disposal is from  $G\alpha RIF$  - it is able to bind to the live S1.2R infected erythrocyte surface and disrupt blood group A rosettes<sup>1</sup>.  $G\alpha RIF$  antibodies show only one band in Western blots of S1.2R lysate and are highly specific to S1.2R when used in live cell surface staining; no labeling of any other tested parasite lines has been observed to date. Based on the peptide array, the reactivity of  $G\alpha RIF$  antibodies was also primarily towards the RIFINs but with some cross-reactivity to other surface antigens. This could be because a much longer full length RIFIN was used in the immunization (as opposed to a peptide antigen in the case of  $R\alpha RIF_C$  and  $R\alpha RIF_I$ ) and may have consequently yielded a greater diversity of antibodies with increased cross-reactivity. This would also explain why multiple bands feature prominently on several parasites' SDS extracts that are beyond the expected sizes of the RIFINs. Notwithstanding, there were five main epitopes spread across the protein length, of which three were unique to the RIFIN used in the immunization (PF3D7\_0100400). Only one epitope with the sequence DRT(T/S/A)QRF (located extracellularly in the first half of the EF-hand domain) reacted against a quarter of all the RIFINs arrayed.

Having validated the specificities of the antibodies and shortlisted four additional parasite strains that were likely to be RIFIN-positive (positive by Western and IFA using  $R\alpha RIF_C$ ), we proceeded with RNA sequencing of two of these strains with the IT4 background to identify which one/ones of the 150–200 *rifs* was expressed. As a surface exposed antigen susceptible to immune recognition, the *rifs* are believed to be expressed in an allelic exclusive manner. This has been demonstrated in the S1.2R transcriptome which showed a single dominantly-expressed *rif* (PFIT\_bin05750)<sup>1</sup>. In this study, we observe that two additional RIFIN-positive parasite lines also transcribe a single dominant *rif*. In FCR3CSA, the *rif* transcript with the highest RPKM value was PFIT\_bin00500, with a value of 2693 that was almost 10-fold higher than the next highest (PFIT\_0536600 with RPKM of 281). Similarly, another single dominant *rif* was found in IT4CD36ICAM1, with PFIT\_0835500 having a RPKM value of 3273 that was almost four-fold higher than the next highest *rif* transcript. The peak expression of these dominant *rif* transcripts all occurred at 20 hpi, suggesting that their protein products may be relevant in the mature asexual parasite stages. In comparison, the two parasite strains that were likely to be RIFIN-negative (negative by Western and IFA using  $R\alpha RIF_C$ ) were also sent for RNA sequencing and both showed much lower RPKM values for all *rifs* at 20 hpi (all *rif* RPKM below 500).

Like the dominant *rif* of S1.2R, the dominant *rif* of FCR3CSA and IT4CD36ICAM1 both have C-terminal sequences containing the motif KKKLQYIK (Supplementary Table S2). This motif was also present on the antigen used for immunizing R $\alpha$ RIF<sub>C</sub> and shown to be an epitope region by the ultra-dense peptide array. This therefore explains the reactivity of R $\alpha$ RIF<sub>C</sub> IgG to the dominant RIFINs of S1.2R, FCR3CSA and IT4CD36ICAM1 by Western blot and IFA. Although the same motif is present on the 'dominant' (highest RPKM at 20 hpi) *rif* of S1.2NR, it is likely that the relatively low RPKM value (13% and 16% of the RPKM of dominant *rif* of FCR3CSA and IT4CD36ICAM1 respectively) and correspondingly lower protein levels resulted in a lack of detection. The 'dominant' *rif* of NF54CSA does not have this motif and was not expected to be reactive.

The sequences of the dominant RIFINs of FCR3CSA and IT4CD36ICAM1 were aligned with the two previously studied RIFINs (PFIT\_bin05750 and PFIT\_3D7\_0100400) using Clustal Omega (Supplementary Figure S3). Using the predictor of apparent free energy difference,  $\Delta G_{app}$  (<http://dgpred.cbr.su.se>)<sup>31</sup> PFIT\_bin00500 and PFIT\_0835500 were predicted to contain 3 possible transmembrane regions: the signal peptide, the hydrophobic patch and transmembrane (TM) domain.

Located upstream from the PEXEL motif, the signal peptides of PFIT\_0835500 and PFIT\_bin00500 have  $\Delta G_{app}$  value of 2.71 and 2.87 respectively. This is slightly higher than the predicted  $\Delta G_{app}$  values of the signal peptide of 3D7\_0100400 and PFIT\_bin05750 (2.22 and 2.53 respectively). The latter two have been shown experimentally to integrate into the ER membrane to at least 70% in an N<sub>cyt</sub>-C<sub>lum</sub> orientation (manuscript in preparation) and it is possible that the signal peptide of PFIT\_0835500 and PFIT\_bin00500 will be inserted likewise. Nevertheless, such signal sequences in *Plasmodium* have proved difficult to predict reliably<sup>32</sup>.

Both PFIT\_bin00500 and PFIT\_0835500 have predicted hydrophobic patches. Though these moderately hydrophobic regions that can be forced into the ER membrane by neighboring TM regions<sup>33</sup>, our recent findings suggest that they are more likely to act as a reentrant loop or could interact with other molecules (manuscript in preparation).

To our knowledge, all RIFINs have a highly hydrophobic TM domain with positive charges on the C-terminal side. PFIT\_bin00500 and PFIT\_0835500 are no exception, and this arrangement would result in the highly conserved C-terminal end of the RIFINs being intracellular and protected from antibody recognition.

The highest PfEMP1 expression for IT4CD36ICAM1 is PFIT\_0811500. While being on the same chromosome (Chr8) as the dominantly expressed RIFIN (PFIT\_0835500), these sequences are about a million bases apart. Based on the genome of the IT4 parasite, the downstream RIFIN gene to PFIT\_0811500 is PFIT\_0811700 (annotated as a RIFIN pseudogene) while the PfEMP1 upstream of PFIT\_0835500 is PFIT\_0811700. This may suggest that the RIFIN most actively transcribed may not necessarily be "paired" with the highest transcribed PfEMP1. As the other dominant *rifs* identified to date (PFIT\_bin05750 and PFIT\_bin00500) have not been mapped to a particular chromosome, it is difficult to speculate further on this possible co-expression of neighbouring *rif* and *var* genes but future identification studies will shed more light on this subject.

The finding that RIFINs may be highly transcribed and expressed in cytoadhesive (but non-rosetting) parasite lines suggests that the role of this highly diverse parasite adhesins are not restricted solely to blood group antigen binding. Future studies alluding to their involvement in other aspects of malaria pathology could yield further insights into the role of malaria in shaping population genetics beyond that of the ABO blood groupings. This study demonstrates the specificity of three polyclonal anti-RIFIN IgG antibodies and reiterates the importance of choosing the right antibodies for the right assays. Given the diversity of RIFIN polymorphisms and the challenges in assaying for them, it is of particular importance that multiple well-validated reagents/techniques be employed to ascertain the presence and involvement of RIFINs in malaria pathology.

## Materials and Methods

**Ethics statement.** Experiments were performed in accordance with relevant guidelines and regulations. Serum and RBCs used for parasite culture were collected from Karolinska Hospital blood bank (ethical permit number: 2009/668-31/3) as approved by the Regional Ethical Review Board in Stockholm, Sweden.

**Parasite culture.** Rosetting *P. falciparum* strains of FCR3S1.2 (S1.2R)<sup>34</sup>, Palo Alto varO (PAvarO)<sup>35</sup> and R29<sup>36</sup>, as well as cultures of non-rosetting FCR3S1.2 (S1.2NR)<sup>1</sup>, NF54CSA<sup>37</sup>, FCR3CSA<sup>37</sup>, 3D7CD36ICAM1<sup>38</sup> and IT4CD36ICAM1<sup>39</sup> were cultured continuously in blood group O+ erythrocytes, grown in media supplemented with 10% A+ sera and synchronized weekly as described elsewhere<sup>1,40</sup>. To minimize the effects of antigenic switching, parasites were cultured for no more than a month after thawing/panning. Cell lines routinely tested negative for mycoplasma contamination.

**SDS extraction of RIFINs and SDS-PAGE.** Cultures of late-stage parasites (35–45 hpi) were first treated with 0.05% saponin and washed twice with PBS to enrich for parasites. The pellet was then resuspended in 1 ml of 0.5% Triton X and spun down hard. The supernatant was discarded and the pellet was resuspended in 2% SDS before being spun down hard again. The SDS extract was then used for SDS-PAGE while the pellet was discarded. The SDS extracts were mixed with 4× NuPAGE LDS loading buffer (Invitrogen) and NuPAGE sample reducing agent (Invitrogen) in 1:15 v/v ratio, heated at 100 °C for 10 min, cooled and loaded into the wells of the pre-cast NuPAGE Novex 4–12% Bis-Tris gels (Invitrogen). NuPAGE MOPS running buffer (Invitrogen) was used, as well as pre-stain plus (Fermentas) protein ladder.

**Antibody production.** The various antigens used in the animal immunizations are listed in Supplementary Table S1 and immunizations were carried out commercially (Agriserä, Vännäs, Sweden) with Freund's incomplete adjuvant. Peptide antigens were coupled to KLH prior to immunization. Serum was harvested after the fourth immunization and IgG purified as described before<sup>1</sup>.



**Western Blot.** Wet-transfer was performed in Tris-glycine transfer buffer (25 mM Tris, 192 mM glycine, 20% MeOH and 0.025% SDS) on a nitrocellulose membrane. Membrane was blocked overnight in 1% Western Blocking Reagent (Roche) in TBS. Labelling was performed at 10 µg/ml of primary antibody with the exception of anti-PfHsp70 (BioSite SPC-186C/D) that was incubated at a 1:2000 dilution. After 1 hr incubation at RT, membranes were washed three times in TBST and incubated with the corresponding HRP-conjugated ECL anti-rabbit IgG (GE Healthcare) or anti-goat IgG (Life Technologies) antibodies (both 1:5000 dilution) for a further 1 hr. After three additional washes with TBST, Amersham ECL prime western blotting detection reagent (GE Healthcare) was added and blots developed on Amersham Hyperfilm ECL (GE healthcare).

**Air dried monolayers preparation, immunofluorescence staining and microscopy.** 15-well (4 mm) glass slides (Thermo Scientific) were pre-treated with poly-L-lysine (0.1 mg/ml, Sigma) for five minutes before being left to dry. Parasite cultures were diluted to 0.1% hematocrit in culture media and 10 µl was added to each well for 30 min. The excess media was removed and the cells left to air dry overnight at RT. Samples were then blocked with 2% BSA for 30 min and primary antibodies (8–10 µg/ml) were added for 1 hr at RT. After washing 3× with PBS, the relevant Alexa488-conjugated secondary antibodies were added for a further 1 hr. After another three washes with PBS, 2 µl of Vectashield with DAPI (Vector laboratories) was added to each well and nail polish was used to seal the coverslip. Cells were visualized with Nikon Eclipse 80i fluorescence microscope under oil-immersion at 100× magnification.

**Peptide array.** Custom ultra-dense peptide microarrays obtained in collaboration with Roche-Nimblegen were applied for epitope region mapping as described before<sup>41,42</sup>. An array containing 175,000 peptides of 12 amino acids in length and with an 11-residue overlap was designed to cover the PfMC2TM family (3D7 and IT background), PHISTs (3D7), RIFINs (3D7 and IT, without pseudogenes), STEVORs (3D7 and IT, without pseudogenes or STEVOR-like proteins), SURFINs (3D7 and IT) and several PfEMP1s (3D7var2csa, ITvar60, ITvar09, PAvAr0, TM284var1, HB3var6, 3D7var4, FCR3S1.6) (Supplementary Data S3). Duplicated (conserved) protein sequences were deleted to reduce the total number of peptides. IgG from non-immune rabbit and goat, as well as IgG from rabbits and a goat immunized with various RIFIN peptides/proteins (Supplementary Table S1), were added to individual peptide arrays. Binding analysis of anti-RIFIN antibodies and also control antibodies occurred via secondary Alexa Fluor 647-conjugated anti-goat IgG or DyLight649-conjugated anti-rabbit IgG (both Jackson ImmunoResearch) and slide scanning at 2 µm resolution (MS200, Roche NimbleGen Inc., Madison, WI). Each spot on the array was subjected to pre-filtration criteria (detailed in a submitted manuscript) to define reactivity and also minimize false positives: by requiring the spot MFI to be above two times the local spot background MFI and maximum 50% coefficient of variation within the spot. Since the peptides have one amino acid lateral shift between adjacent peptides, if at least two adjacent reactive peptides were reactive, the region (epitope) was regarded bona fide (i.e. requiring a maximum minimal epitope of 11 amino acids). Thus, any reactive peptide with no reactivity on either adjacent peptide was excluded to minimize the number of potential false-positives arising from non-specific binding. The total number of peptides belonging to an epitope region was then used to score the likelihood of specific interaction between the serum-derived polyclonal IgG and various parasite proteins; here termed “reactivity score” for convenience.

**RNA extraction.** Synchronized parasite cultures were staged by Giemsa thin smears and harvested at 10, 20, 30 and 40 hpi. For every 100 µl of packed cells, 1 ml of TRIzol reagent (Ambion) was used and the aqueous phase was retained after mixing with chloroform and centrifugation. A second phase separation was performed by addition of acid phenol chloroform (1:1 v/v ratio) following the manufacturer's recommendations. Precipitation of RNA was done using isopropanol and the pellet was eventually dissolved in RNase-free water and stored at –80 °C.

**RNA sequencing.** The extracted RNA was then checked for quality in Bio-analyzer (Agilent) and 2 µg of RNA used to construct sequence library using TruSeq Stranded mRNA Library Prep kit (Illumina). Sequencing was performed on the Illumina HiSeq 2000 platform to obtain 2 × 100 bp paired-end reads. Reads were aligned to the corresponding reference genomes using Star and HTSeq. NF54CSA was aligned to the 3D7 genome while S1.2NR, FCR3CSA and IT4CD36ICAM1 were aligned to the IT4 genome obtained from www.plasmoDB.org. Results are presented here in Reads Per Kilobase of transcript per Million mapped reads (RPKM).

**Quantitative Real-Time PCR (qPCR).** Total RNA was extracted at 20 hpi, DNase treated (Ambion) and reverse transcribed (iScript<sup>TM</sup>, Bio-Rad) according to manufacturer's instructions. Triplicate amplification reactions were performed for each gene with a mix of 1 µl cDNA, 1 × SYBR green mix (PowerUp<sup>TM</sup>, Life Technologies) and 500 nM of both forward and reverse primer (Supplementary Table S3). The program used was as follows 95 °C for 3 min, 50 × at 95 °C for 10 s, 60 °C for 30 s with the data recorded at the elongation step. Data was analyzed by computing efficiency corrected relative quantities using the *fructose-bisphosphate aldolase* (FBA, PFIT\_1446000) as reference gene and the S1.2NR parasite used as a calibrator (software used: Bio-Rad CFX Manager 2.1). qPCR based relative quantities (RQ) for all time points and genes were thereafter plotted against fold-changes obtained by RNA sequencing and a correlative index was computed by Pearson's R.

## References

- Goel, S. *et al.* RIFINs are adhesins implicated in severe Plasmodium falciparum malaria. *Nat Med* **21**, 314–317, doi: 10.1038/nm.3812 (2015).
- Gardner, M. J. *et al.* Genome sequence of the human malaria parasite Plasmodium falciparum. *Nature* **419**, 498–511, doi: 10.1038/nature01097 (2002).

3. Joannin, N., Abhiman, S., Sonnhammer, E. L. & Wahlgren, M. Sub-grouping and sub-functionalization of the RIFIN multi-copy protein family. *BMC Genomics* **9**, 19, doi: 10.1186/1471-2164-9-19 (2008).
4. Cheng, Q. *et al.* *stevor* and *rif* are Plasmodium falciparum multicopy gene families which potentially encode variant antigens. *Mol Biochem Parasitol* **97**, 161–176 (1998).
5. Helmby, H., Cavelier, L., Pettersson, U. & Wahlgren, M. Rosetting Plasmodium falciparum-infected erythrocytes express unique strain-specific antigens on their surface. *Infect Immun* **61**, 284–288 (1993).
6. Haeggstrom, M. A., V. O. N. E., Kironde, F., Fernandez, V. & Wahlgren, M. Characterization of Maurer's clefts in Plasmodium falciparum-infected erythrocytes. *Am J Trop Med Hyg* **76**, 27–32 (2007).
7. Bachmann, A. *et al.* Temporal expression and localization patterns of variant surface antigens in clinical Plasmodium falciparum isolates during erythrocyte schizogony. *PLoS One* **7**, e49540, doi: 10.1371/journal.pone.0049540 (2012).
8. Petter, M. *et al.* Variant proteins of the Plasmodium falciparum RIFIN family show distinct subcellular localization and developmental expression patterns. *Mol Biochem Parasitol* **156**, 51–61, doi: 10.1016/j.molbiopara.2007.07.011 (2007).
9. Wang, C. W., Magistrado, P. A., Nielsen, M. A., Theander, T. G. & Lavstsen, T. Preferential transcription of conserved *rif* genes in two phenotypically distinct Plasmodium falciparum parasite lines. *Int J Parasitol* **39**, 655–664, doi: 10.1016/j.ijpara.2008.11.014 (2009).
10. Mwakalinga, S. B. *et al.* Expression of a type B RIFIN in Plasmodium falciparum merozoites and gametes. *Malar J* **11**, 429, doi: 10.1186/1475-2875-11-429 (2012).
11. Fischer, P. R. & Boone, P. Short report: severe malaria associated with blood group. *Am J Trop Med Hyg* **58**, 122–123 (1998).
12. Lell, B. *et al.* The role of red blood cell polymorphisms in resistance and susceptibility to malaria. *Clin Infect Dis* **28**, 794–799, doi: 10.1086/515193 (1999).
13. Pathirana, S. L. *et al.* ABO-blood-group types and protection against severe, Plasmodium falciparum malaria. *Ann Trop Med Parasitol* **99**, 119–124, doi: 10.1179/136485905X19946 (2005).
14. Loscertales, M. P. & Brabin, B. J. ABO phenotypes and malaria related outcomes in mothers and babies in The Gambia: a role for histo-blood groups in placental malaria? *Malar J* **5**, 72, doi: 10.1186/1475-2875-5-72 (2006).
15. Rowe, J. A. *et al.* Blood group O protects against severe Plasmodium falciparum malaria through the mechanism of reduced rosetting. *Proc Natl Acad Sci USA* **104**, 17471–17476, doi: 10.1073/pnas.0705390104 (2007).
16. Fry, A. E. *et al.* Common variation in the ABO glycosyltransferase is associated with susceptibility to severe Plasmodium falciparum malaria. *Human molecular genetics* **17**, 567–576, doi: 10.1093/hmg/ddm331 (2008).
17. Carlson, J. & Wahlgren, M. Plasmodium falciparum erythrocyte rosetting is mediated by promiscuous lectin-like interactions. *J Exp Med* **176**, 1311–1317 (1992).
18. Carlson, J., Nash, G. B., Gabutti, V., al-Yaman, F. & Wahlgren, M. Natural protection against severe Plasmodium falciparum malaria due to impaired rosette formation. *Blood* **84**, 3909–3914 (1994).
19. Ching, J. H. *et al.* Rosette-Disrupting Effect of an Anti-Plasmodial Compound for the Potential Treatment of Plasmodium falciparum Malaria Complications. *Sci Rep* **6**, 29317, doi: 10.1038/srep29317 (2016).
20. Moll, K., Palmkvist, M., Ching, J., Kiwuwa, M. S. & Wahlgren, M. Evasion of Immunity to Plasmodium falciparum: Rosettes of Blood Group A Impair Recognition of PfEMP1. *PLoS One* **10**, e0145120, doi: 10.1371/journal.pone.0145120 (2015).
21. Tan, J. *et al.* A LAIR1 insertion generates broadly reactive antibodies against malaria variant antigens. *Nature* **529**, 105–109, doi: 10.1038/nature16450 (2016).
22. Fernandez, V., Hommel, M., Chen, Q., Hagblom, P. & Wahlgren, M. Small, clonally variant antigens expressed on the surface of the Plasmodium falciparum-infected erythrocyte are encoded by the *rif* gene family and are the target of human immune responses. *J Exp Med* **190**, 1393–1404 (1999).
23. Abdel-Latif, M. S., Khattab, A., Lindenthal, C., Krensner, P. G. & Klinkert, M. Q. Recognition of variant Rifin antigens by human antibodies induced during natural Plasmodium falciparum infections. *Infect Immun* **70**, 7013–7021 (2002).
24. Khattab, A. & Klinkert, M. Q. Maurer's clefts-restricted localization, orientation and export of a Plasmodium falciparum RIFIN. *Traffic* **7**, 1654–1665, doi: 10.1111/j.1600-0854.2006.00494.x (2006).
25. Bachmann, A. *et al.* A comparative study of the localization and membrane topology of members of the RIFIN, STEVOR and PfMC-2TM protein families in Plasmodium falciparum-infected erythrocytes. *Malar J* **14**, 274, doi: 10.1186/s12936-015-0784-2 (2015).
26. Kyes, S. A., Rowe, J. A., Kriek, N. & Newbold, C. I. Rifins: a second family of clonally variant proteins expressed on the surface of red cells infected with Plasmodium falciparum. *Proc Natl Acad Sci USA* **96**, 9333–9338 (1999).
27. Haeggstrom, M. *et al.* Common trafficking pathway for variant antigens destined for the surface of the Plasmodium falciparum-infected erythrocyte. *Mol Biochem Parasitol* **133**, 1–14 (2004).
28. Baker, M. Reproducibility crisis: Blame it on the antibodies. *Nature* **521**, 274–276, doi: 10.1038/521274a (2015).
29. Uhlen, M. *et al.* A proposal for validation of antibodies. *Nature methods* **13**, 823–827, doi: 10.1038/nmeth.3995 (2016).
30. Blomqvist, K. *et al.* A sequence in subdomain 2 of DBL1alpha of Plasmodium falciparum erythrocyte membrane protein 1 induces strain transcending antibodies. *PLoS One* **8**, e52679, doi: 10.1371/journal.pone.0052679 (2013).
31. Hessa, T. *et al.* Molecular code for transmembrane-helix recognition by the Sec61 translocon. *Nature* **450**, 1026–1030, doi: 10.1038/nature06387 (2007).
32. Nacer, A., Berry, L., Slomianny, C. & Mattei, D. Plasmodium falciparum signal sequences: simply sequences or special signals? *Int J Parasitol* **31**, 1371–1379 (2001).
33. Ojemalm, K., Halling, K. K., Nilsson, I. & von Heijne, G. Orientational preferences of neighboring helices can drive ER insertion of a marginally hydrophobic transmembrane helix. *Mol Cell* **45**, 529–540, doi: 10.1016/j.molcel.2011.12.024 (2012).
34. Albrecht, L. *et al.* var gene transcription and PfEMP1 expression in the rosetting and cytoadhesive Plasmodium falciparum clone FCR3S1.2. *Malaria journal* **10**, 17, doi: 10.1186/1475-2875-10-17 (2011).
35. Rowe, J. A., Moulds, J. M., Newbold, C. I. & Miller, L. H. P. falciparum rosetting mediated by a parasite-variant erythrocyte membrane protein and complement-receptor 1. *Nature* **388**, 292–295, doi: 10.1038/40888 (1997).
36. Vigan-Womas, I. *et al.* An *In Vivo* and *In Vitro* Model of Plasmodium falciparum Rosetting and Autoagglutination Mediated by varO, a Group A var Gene Encoding a Frequent Serotype. *Infection and Immunity* **76**, 5565–5580, doi: 10.1128/iai.00901-08 (2008).
37. Rasti, N. *et al.* Nonimmune immunoglobulin binding and multiple adhesion characterize Plasmodium falciparum-infected erythrocytes of placental origin. *Proceedings of the National Academy of Sciences* **103**, 13795–13800, doi: 10.1073/pnas.0601519103 (2006).
38. Gölnitz, U., Albrecht, L. & Wunderlich, G. Var transcription profiling of Plasmodium falciparum 3D7: assignment of cytoadherent phenotypes to dominant transcripts. *Malaria journal* **7**, 14, doi: 10.1186/1475-2875-7-14 (2008).
39. McCormick, C. J., Craig, A., Roberts, D., Newbold, C. I. & Berendt, A. R. Intercellular adhesion molecule-1 and CD36 synergize to mediate adherence of Plasmodium falciparum-infected erythrocytes to cultured human microvascular endothelial cells. *The Journal of clinical investigation* **100**, 2521–2529, doi: 10.1172/jci119794 (1997).
40. Moll, K., Kaneko, A., Scherf, A. & Wahlgren, M. *Methods in Malaria Research (6th Edition)*. (EviMalaR, Glasgow, UK & MR4/ATCC, Manassas, VA, USA, 2013, 2014).
41. Forsstrom, B. *et al.* Proteome-wide epitope mapping of antibodies using ultra-dense peptide arrays. *Mol Cell Proteomics* **13**, 1585–1597, doi: 10.1074/mcp.M113.033308 (2014).
42. Qundos, U. *et al.* Affinity proteomics discovers decreased levels of AMFR in plasma from Osteoporosis patients. *Proteomics Clin Appl* **10**, 681–690, doi: 10.1002/prca.201400167 (2016).

## Acknowledgements

This study was supported by the Swedish Strategic Foundation (SB12-0026.005) and the Swedish Research Council (VR/2012-2016/521-2011-3377). JHC is supported by Swedish Strategic Foundation and National University of Singapore. Authors wish to thank Ulf Ribacke for input on qPCR analyses, Mia Palmqvist for input on antibody characterization and also Thomas Kallman from the Bioinformatics Services to Swedish Life Science (BILS) for RNAseq analyses. RNAseq computations were performed on resources provided by the Swedish National Infrastructure for Computing (SNIC) at Uppsala Multidisciplinary Center for Advanced Computational Science (UPPMAX). High-density peptide arrays were provided by Protein and Peptide Arrays, SciLifeLab.

## Author Contributions

Study design: J.H.C. and M.W.; Western blot, IFA, RNA extraction: J.H.C.; qPCR: M.S.; peptide array design, experiments and analyses: A.Z., U.Q., P.N., J.H.C., M.d.P.Q. and K.M.; RNAseq: J.H.C., M.d.P.Q. and S.C.L.C.; RIFIN sequence analyses: A.T.-R. and I.N.; manuscript preparation: all authors.

## Additional Information

**Supplementary information** accompanies this paper at <http://www.nature.com/srep>

**Competing financial interests:** MW is a co-founder and board member of Modus Therapeutics AB, a company developing drugs for severe malaria. All other authors declare no financial conflicts of interest.

**How to cite this article:** Ch'ng, J.-H. *et al.* Epitopes of anti-RIFIN antibodies and characterization of *rif*-expressing *Plasmodium falciparum* parasites by RNA sequencing. *Sci. Rep.* 7, 43190; doi: 10.1038/srep43190 (2017).

**Publisher's note:** Springer Nature remains neutral with regard to jurisdictional claims in published maps and institutional affiliations.



This work is licensed under a Creative Commons Attribution 4.0 International License. The images or other third party material in this article are included in the article's Creative Commons license, unless indicated otherwise in the credit line; if the material is not included under the Creative Commons license, users will need to obtain permission from the license holder to reproduce the material. To view a copy of this license, visit <http://creativecommons.org/licenses/by/4.0/>

© The Author(s) 2017